Reduced enteric BDNF-TrkB signaling drives glucocorticoid-mediated GI dysmotility

Jared Slosberg[1#], Srinivas N. Puttapaka[2#], Philippa Seika[2], Su Min Hong[2], Alpana Singh[3], Subhash Kulkarni[2, 5, 6*]

[1]Department of Genetic Medicine, Johns Hopkins University – School of Medicine, Baltimore, MD, USA

[2]Division of Gastroenterology, Dept of Medicine, Beth Israel Deaconess Medical Center, Boston, MA 02115

[3]Cleveland Clinic, Cleveland

[4]Department of Oncology, Johns Hopkins University – School of Medicine, Baltimore, MD, USA

[5]Division of Medical Sciences, Harvard Medical School, Boston, MA 02115

[6]Graduate program in Neuroscience, Harvard Medical School, Boston, MA 02115

[#]Joint first co-authors

*Address all correspondence to:

Subhash Kulkarni, Ph.D.

skulkar1@bidmc.harvard.edu

Abstract:

Stress affects gastrointestinal (GI) function causing dysmotility, especially in *disorders of gut-brain interactions (DGBI)* patients. GI motility is regulated by the enteric nervous system (ENS), suggesting that stress alters ENS biology to cause dysmotility. While stress increases glucocorticoid levels through the hypothalamus-pituitary-adrenal axis, how glucocorticoids affect GI motility is not known. Glucocorticoid signaling reduces expression of specific transcriptional isoforms of brain-derived neurotrophic factor (BDNF) in the central nervous system, altering signaling through its receptor Tropomyosin-related kinase B (TrkB) to cause behavioral defects. However, since the nature of ENS-specific *Bdnf* isoforms and their response to glucocorticoids remains unknown, we are limited in studying how stress impacts the ENS to cause dysmotility. Here, in male and female mice, we establish that stress-responsive *Bdnf* isoforms that are transcriptionally regulated at exons 4 and 6 represent >85% of all *Bdnf* isoforms in the post-natal ENS, and that *Bdnf* and *Ntrk2* (TrkB) are expressed by enteric neurons. We further show using male mice dosed with a synthetic glucocorticoid receptor (GR) agonist dexamethasone (Dexa), that increased glucocorticoid signaling in ENS significantly reduces the expression of *Bdnf* transcripts and protein and that it significantly reduces GI motility. Finally, by using HIOC, a specific synthetic agonist of TrkB, we observe that HIOC treatment significantly improved GI motility of a cohort of Dexa-treated male mice, when compared to Dexa-treated and HIOC-untreated mice. Our results implicate BDNF- TrkB signaling in the etiology of stress-associated dysmotility and suggest that TrkB is a putative therapeutic target for dysmotility in DGBI patients.

Significance statement:

The mechanism through which stress-associated increase in glucocorticoid signaling causes gastrointestinal (GI) dysmotility is not well understood. GI motility is regulated by the enteric nervous system, which depends on optimal signaling between brain-derived neurotrophic factor (BDNF) and its receptor tropomyosin related kinase B (TrkB). The lack of clarity on whether glucocorticoid impact BDNF signaling in the ENS, analogous to the manner they affect BDNF in brain, has limited our understanding of stress-associated dysmotility. Here, by identifying the nature of *Bdnf* isoforms expressed in ENS, studying their response to increased glucocorticoid signaling, and testing the effect of TrkB agonist to promote healthy gut motility in a model of glucocorticoid-driven dysmotility, we implicate altered BDNF-TrkB signaling as the mechanism driving stress-associated dysmotility.

Introduction:

Stress-associated gastrointestinal (GI) dysmotility afflicts large numbers of patients and is an important factor in the development of irritable bowel syndrome (IBS) (Qin et al., 2014; Sperber et al., 2021; Leigh et al., 2023). GI motility is regulated by the enteric nervous system (ENS) (Wood, 2016), suggesting that stress-associated GI dysmotility occurs due to ENS dysfunction. Healthy ENS function relies on optimal neurotrophin signaling, which include interactions between neurotrophins, which are secreted by diverse gut cell types, and their specific receptor that is expressed by ENS neurons (Liu, 2018; Chalazonitis et al., 2020; Sharkey and Mawe, 2023). Brain-derived neurotrophic factor (BDNF) and its receptor tropomyosin kinase B (TrkB, coded by *Ntrk2*) constitutes one such significant neurotrophin system known to regulate neuronal signaling in the central nervous system (CNS) (Martinowich et al., 2007). Stress also causes significant changes in CNS neuronal function resulting in significant and observable changes in behavior (Zheng et al., 2024), and stress-induced reductions in BDNF expression and hence BDNF–TrkB signaling is known to be a significant mechanism through which stress affects CNS function (Begni et al., 2016). However, whether a similar BDNF-dependent mechanism drives stress-associated GI dysmotility is not known.

Studies on rodent models of health and disease have informed that BDNF regulates GI motility as its presence accelerates gastrointestinal transit, likely through a combination of its neuromodulatory role and more direct effects on the excitatory potential of the muscularis externa (Boesmans et al., 2008; Chen et al., 2012; Chen et al., 2014; Singh et al., 2020). This prokinetic effect of BDNF observed in rodents appears to translate to slow-transit constipation (STC) patients, as decreased BDNF presence was detected in colonic tissues from this cohort (Chen et al., 2014) and exogenous BDNF supplementation restored intestinal transit measures in constipated patients (Coulie et al., 2000). These data suggest that mechanisms regulating BDNF levels are important for the pathobiology of GI dysmotility. Further, significant alterations in *Bdnf* transcript levels in distressed IBS patients (Konturek et al., 2020; Zhang et al., 2021) suggest that this regulation may extend to stress-induced GI dysmotility. However, how stress affects enteric BDNF and TrkB and if stress-induced reduction in enteric BDNF levels and BDNF–TrkB signaling mediate the development of GI dysmotility is not known.

BDNF levels are regulated at the level of transcription. The *Bdnf* gene consists of nine exons of which the first 8 are non-coding exons (e1 – e8) that are transcribed but not translated, and only the 9th exon (e9) contains the translated coding sequence (Aid et al., 2007). Transcription results

in *Bdnf* isoforms containing any one of the eight e1 – e8 exons spliced to the protein coding exon e9. The non-coding exons each provide alternative transcription start sites for *Bdnf* isoforms, and each non-coding exon contains an exon-specific promoter sequence that is differentially regulated (Aid et al., 2007). Variation in promoter usage allows for context-dependent regulation of *Bdnf* expression, as has been demonstrated for activity-dependent synaptic plasticity in the CNS (Hong et al., 2008; Pruunsild et al., 2011). Additionally, physiological stress has been implicated as a potent regulator of *Bdnf* expression and abundance (Murakami et al., 2005; Tsankova et al., 2006; Hill and Martinowich, 2016; Linz et al., 2019). Stress manifests its many effects on viscera through the hypothalamic-pituitary-adrenal (HPA) axis, whereby corticotropin-releasing hormone (CRH) released by hypothalamic neurons in response to stress induces the release of adrenocorticotropic hormone (ACTH) from pituitary. This, in turn, directs the adrenal glands to release the glucocorticoid hormone cortisol (Russell and Lightman, 2019). Chen et al.(Chen et al., 2017) observed that Glucocorticoids (GCs) specifically repress the expression of *Bdnf* isoforms IV (transcription from promoter of *Bdnf*-e4) and VI (transcription from promoter of *Bdnf*-e6) by binding to the glucocorticoid responsive elements (GREs) in e4 and e6 promoter sequences. While the effect of both stress and glucocorticoid supplementation on altering gut motility in adult mice has been observed (Schneider et al., 2023), whether stress-associated GI dysmotility is driven by a similar glucocorticoid-mediated repression of *Bdnf* in the ENS is not known. This lack of understanding has been driven by a lack of clarity on the nature of BDNF and TrkB-expressing cells in the gut wall, the nature of *Bdnf* isoform expression and their susceptibility to glucocorticoid stimulation in the adult ENS, and whether stimulating TrkB signaling reverts the effect of glucocorticoid-induced GI dysmotility.

To address these gaps in the field, here, we further our mechanistic understanding of stress-associated GI dysmotility by using immunofluorescence, RNAScope, bulk transcriptomic, and quantitative PCR-based assays to study the expression of BDNF and TrkB in the gut wall tissue containing myenteric neurons. Further, we used restraint stress and a synthetic glucocorticoid receptor agonist Dexamethasone to assess how stress and glucocorticoid receptor stimulation influence BDNF levels to drive dysmotility. Finally, we test whether stimulating BDNF-TrkB signaling promotes healthy GI motility in a mouse model of glucocorticoid-induced GI dysmotility. Our results show that both BDNF and TrkB are expressed by adult enteric neurons, and that stress-responsive isoforms of *Bdnf* represent the majority of all *Bdnf* isoforms in the post-natal myenteric plexus tissue. We find that dexamethasone exposure causes a significant reduction in BDNF protein levels, driven by a significant reduction in expression of the stress-responsive *Bdnf*

isoforms, and that dexamethasone-induced abnormalities in GI motility can be reversed by stimulating TrkB signaling using a specific TrkB agonist HIOC.

Methods

Human tissue procurement and immunohistochemistry: Paraffin sections of the adult small intestinal full-thickness gut from deidentified human tissues were obtained from the Department of Pathology at Beth Israel Deaconess Medical Center, and the Institutional Review Board approved using the deidentified human tissues. Antigen retrieval was performed on 5 um thick sections at 97ºC for 40 minutes using citrate buffer at pH 6.0, followed by immunostaining with anti-BDNF antibody (abcam, Cat. No. ab108319, dilution 1:500). The tissue sections were then counterstained with DAB chromogen staining, mounted with Cytoseal, and imaged under 40X brightfield. Microscopy was performed using the Nikon Eclipse Ni-U Upright microscope with 40x Nikon Plan Fluor objective. Images were acquired using the Nikon DS-Fi3 camera and NIS-Elements BR software (Version 5.20.01). During image acquisition, exposure time was adjusted using the Color DS-Fi3 settings to obtain a clear definition of tissue structure. Images were acquired in the TIFF format.

Animals: We used male and female wildtype C57BL/6J mice from the National Institute on Aging colony (at the ages of 1, 6, and 17 months) for the bulk RNA sequencing experiment. For all other experiments, we used adult male wildtype C57BL/6J mice (between the ages of 12 and 20 weeks) from the National Institute on Aging colony. Mice were housed in a controlled environment under a 12 h light/dark cycle at 22 ± 2℃, 55 ± 5% humidity with access to food and water ad libitum. All animal procedures were carried out strictly under protocols approved by the Animal Care and Use Committee of Johns Hopkins University and of Beth Israel Deaconess Medical Center (BIDMC) in accordance with the guidelines provided by the National Institutes of Health.

Bulk RNA sequencing (bulkRNA-seq) experiments:

Tissue Isolation for bulkRNA-seq: Mice of three ages (1-month, 6-month, and 17-month) and both sexes (n=3 per unique condition) were anesthetized with isoflurane and sacrificed by cervical dislocation. For small intestinal tissue isolation, a laparotomy was performed, and the entire small intestine was removed and flushed with ice-cold nuclease-free 1X PBS. The ileum, defined as the distal third of the small intestine, was cut into 3 cm sections for peeling. Next, tissues were placed over a sterile plastic rod and a superficial longitudinal incision was made along the serosal surface and the longitudinal muscle containing myenteric plexus (LM-MP) was peeled off from the underlying tissue using a wet sterile cotton swab. Each gut muscle strip was immediately flash

frozen in liquid nitrogen before storage at -80°C. The average time from sacrifice to flash freeze was 10 minutes. Animals were processed in three batches, balanced across age/sex composition and order of processing.

Library Prep & Sequencing: RNA isolation, library preparation, and sequencing were completed at the JHU Single Cell and Transcriptomic Core. Samples with RIN >= 7.0 were used for library preparation, with all samples being high-quality except one 17-month female (resulting n=2, average RIN of 17 samples that passed this threshold > 9.0). Frozen tissue samples each in 1.5mL tubes were submerged in 375 uL of RLT buffer with β-mercaptoethanol. Tissue and buffer were transferred to a ice-cold 2 mL Qiagen sample tube with a 5mm stainless steel bead and lysed in a TissueLyzer at full speed for 3 minutes. RNA isolation was completed with the Qiagen RNeasy Mini, Animal Tissue and Cells with DNA Digest protocol. cDNA libraries were prepared with the TruSeq Stranded mRNA Library Prep with unique dual indexes. Paired-end (2x-50bp) sequencing was completed on a NovaSeq 6000 system.

Preprocessing: Isoform-level transcript abundances were estimated by pseudoalignment via Kallisto 'quant' (version 0.48.0) to the GENCODE vM27 reference genome assembly. Default parameters were used, except the number of bootstraps was set to 100 to estimate uncertainty ("-b 100"). The median fragment length, as estimated by Kallisto, was 168.7 base pairs. Across all sequenced samples, the median number of reads per sample was 46,756,241 (range: 34.6 M to 58.2 M) and 94.2% of reads were successfully pseudoaligned to the reference.

Quality control & analysis: For quality control analyses, isoforms were collapsed to gene-level and abundances were normalized by the "scaledTPM" option within tximport, and further analyzed with DESeq2 (v1.30.1, R v4.0.2). Genes were removed from the analysis if they had fewer than 10 counts across all samples or were not detected in at least three samples. At the sample level, PCA and Cook's distance were used to identify potential outliers. Both approaches identified one 17-month male sample as a source of outlier expression, and this sample also had the lowest RIN (7.0). With this outlier sample removed, isoform-level abundances of the remaining 16 samples were analyzed with IsoformSwitchAnalyzeR (v2.1.2, R v4.2).

Restraint stress model: Adult male mice were divided into two cohorts, control and stressed. Mice in stressed cohorts were restrained for 1 hour every day for 5 consecutive days and were then released back into their cages. The timing of the restraint during the day was varied across the 5 days to reduce habituation. By contrast, the mice in the control group were handled similarly, but were not restrained and were returned to the cage immediately after handling. The whole gut

transit time (WGTT) of the mice in response to treatment was assayed on the day after the last day of restraint.

Dexamethasone induced model of GI dysmotility: Adult male mice were divided into two cohorts, control and DEXA. Mice in the control group were treated with vehicle (10% DMSO in saline, intraperitoneal route) and those in the DEXA group were treated with dexamethasone (MedChemExpress, Cat. No. HY-14648; 5mg/kg in 10% DMSO/body weight, intraperitoneal route) group. Dexamethasone is light sensitive so was shielded from bright light, both in powder form and in solution. Mice were first housed in individual cages and after a habituation phase lasting 30min, they were treated with vehicle or dexamethasone, which were administered intraperitoneally using a sterile 1 ml insulin syringe. The mice were subjected to WGTT assays 30 minutes after the treatment.

Another 2 cohorts of mice were similarly used, wherein one the control cohort was dosed similarly with vehicle and the DEXA group was dosed similarly with dexamethasone. 4 hours after the treatment, the mice were sacrificed, and their small intestinal LM-MP tissues were isolated and immediately snap-frozen in liquid nitrogen.

Effect of TrkB agonist HIOC on dexamethasone-induced model of GI dysmotility: HIOC (N-[2-(5-hydroxy-1H-indol-3-yl)ethyl]-2-oxopiperidine-3-carboxamide) is a known specific agonist of TrkB. Adult male mice were divided into two cohorts, DEXA and DEXA+HIOC. Mice were first housed in individual cages and then those in the DEXA+HIOC group were treated with HIOC (MedChemExpress, Cat. No. HY-101446; 50 mg/kg in 10% DMSO/body weight, intraperitoneal route), while those in DEXA group were treated with Vehicle (10% DMSO in saline, intraperitoneal route). The mice were then released back to their individual cages for 30 minutes after which both groups were treated with DEXA (50 mg/kg in 10% DMSO/body weight, intraperitoneal route) and again released back to their individual cages for an additional 30 minutes. Treatment was administered intraperitoneally using a sterile 1 ml insulin syringe. The mice were subjected to whole gut transit time assays 30 minutes after the DEXA treatment.

Whole gut transit time analyses (WGTT): These experiments were started between the times of 8 and 9 AM. Mice were individually caged in plastic cages without bedding and were left undisturbed 30 minutes. Water was provided to the mice before and during the experiment *ad libitum*. All mice received oral gavage of 300 µl of 6% (w/v) carmine red (Sigma C1022) in 0.5% (w/v) methylcellulose (Sigma M0512) in sterile water. The oral gavage was performed such that the entirety of the dye suspension was delivered into the animal's stomach. The mice were then

left undisturbed in their individual cages for 70 minutes after which their cages were checked every 15 minutes for the presence of red colored fecal pellets. The time post-gavage for every mouse to produce a red colored fecal pellet was measured, and the difference between the gavage time and red fecal pellet production time was established as the whole gut transit time for that mouse. The experiment was terminated at 250 minutes post-gavage and the WGTT of any mice that did not expel the red dye at the termination was marked at the value of 265 (i.e. 250 + 15) min. The mean difference in WGTT (in minutes) between cohorts was analyzed statistically.

Mouse small intestine LM-MP tissue isolation for non-sequencing experiments: Mice were anesthetized with isoflurane and sacrificed by cervical dislocation. Mouse placed in dorsal recumbency on the surgical surface, disinfected skin with 70% EtOH then opened the abdominal cavity and collected the small intestine (SI) into a petri dish containing PBS with 1x Pen-Strep. Sterile PBS solution flushed through the intestine using a 20ml syringe to remove fecal matter. Entire small intestine cut into 2cm pieces into a sterile petri dish containing Opti-MEM medium with 1X Pen-Strep. SI segments were placed over a sterile 1ml pipette and LM-MP tissue was peeled off from the underlying tissue using a wet sterile cotton swab. Tissues isolated for qPCR-based assessment of *Bdnf* levels were snap frozen immediately after isolation. Tissues isolated for culture were placed in a fresh sterile ice-cold Opti-MEM medium for further use. Tissues isolated for RNAScope analyses were flattened and cryo-preserved in optimal cutting temperature (OCT) compound (TissueTEK) on dry ice.

In Vitro LM-MP tissue culture and treatments: Isolated LM-MP tissues were placed in a sterile 24 well dish containing Stem cell media (SCM, made up of Neurobasal medium containing L-glutamine, B27, and Pen-Strep (all Invitrogen) and Bovine Serum Albumin (Sigma)(Kulkarni et al., 2017)) and treated with Vehicle (10% DMSO in saline) or Dexamethasone (1μM in 10% DMSO) for 4 hrs. After the incubation, tissues were snap frozen in liquid nitrogen & stored at -80°C for further experimental analysis.

RNA isolation and quantitative real-time PCR: Total RNA was extracted from frozen LM-MP tissues with Direct-zol RNA miniprep kit (Zymo research) and 1 μg RNA was converted to cDNA using SuperScript III (Therno, Cat.No.11752050) in a 20μl reaction. Quantitative real-time PCR was performed on a QuantStudio3 real time PCR system (Life Technologies, USA) with TaqMan Fast advanced qPCR Master Mix (Cat. No. 4444557, Thermo Scientific, USA) using gene specific TaqMan assay probes. Mouse HPRT served as a housekeeping gene for normalization. Primer and probe information is provided in Table 1. 20μl qRT-PCR reactions were incubated at 95 ℃ for

10 min, followed by 40 cycles at 95 ℃ for 10 s, 60℃ for 10 s, and 72 ℃ for 40 s. Relative fold changes of genes between treatment groups were calculated using the $2^{-\Delta\Delta Ct}$ method.

Protein isolation and ELISA: Proteins from frozen LM-MP were extracted using a cell lysis buffer containing RIPA buffer (150 mM NaCl, 50 mM Tris-HCl pH 8.0, 1% NP-40, 0.1% sodium deoxycholate and 0.1% SDS, adjusted with distilled water). Succinctly, for every LM-MP peel, we add 20 µl of 1X RIPA+++ buffer which contains RIPA with Halt Protease Inhibitor (Invitrogen, Cat. No. 78438) at a conc. of 5-10X and Phosphatase Inhibitors 2 and 3 (Sigma Aldrich, Cat. Nos. P5726 and P0044) at a concentration of 2-3% to locking sterile Eppendorf tubes and then add 6-8 sterile autoclaved silicon beads. Tissue was homogenized using bead beater in cold room at 7-8 speed setting for 5 mins, after which the tubes were shaken at 200-250 rpm for 30-40 mins in cold room, centrifuged at over 12,000rpm for 20 mins at 4ºC. Supernatant thus generated was collected to be used for ELISA. The levels of BDNF in the LM-MP tissues cultured with and without dexamethasone were measured using the BDNF DuoSet kit (R&D Systems; DY248). In brief, sterile and clean ELISA-grade 96-well (Corning) were coated with 100 µl of diluted capture antibody/well and incubated overnight at room temperature. On the second day, the plates were washed and blocked with reagent diluent (300 µl for 1 hour at room temperature and 100 µl of protein extract, standards in reagent diluent, or appropriate diluent were added to the prepared wells and incubated for 2 hours at room temperature. Following this, 100 µl each of detection antibody, working dilution of streptavidin-HRP, substrate solution, and 50 µl of stop solution were sequentially added to each well. The optical density of each well was measured using a microplate reader set to 540 nm. The BDNF concentration was expressed in picograms of BDNF per microgram of protein.

RNAScope: 15 µm thick sections of adult murine small intestinal LM-MP tissues that were fresh frozen in OCT were processed for RNAscope® 2.0 assay for labeling and detecting *Bdnf, Ntrk2* (TrkB) and pan-neuronal *Tubb3* transcripts, which was performed using manufacturer's instructions(Wang et al., 2012). The information on the probes used is provided in Table 1. RNAscope® labeling was provided by the Neurobiology Imaging Facility (NIF) at Harvard Medical School, Boston, MA. The tissue sections after labeling were labeled with DAPI (nuclear dye) and mounted with Prolong Gold Anti-fade mountant (Invitrogen) and imaged under Zeiss 880 Confocal microscope using 40X water immersion objective. The images were analyzed with Fiji (ImageJ, NIH).

Results

Restraint stress and glucocorticoid receptor agonism in adult mice slows down whole gut motility. The Thaiss group recently studied the effect of restraint stress on GI motility and found that this physiological stress significantly slows down whole GI motility (Schneider et al., 2023). We recreated this model and found concordance with these results, as restraint stress applied in our adult male C57BL/6 mice also caused a significant slowing of whole gut motility, as assayed by the carmine-red dye method (n = 5/cohort; mean ± S.E. of WGTT (in min): Control: 93.0 ± 5.612; Stress: 123.0 ± 8.746, p = 0.02, Students' t-test; **Fig 1**). Since stress manifests its effects through the HPA axis to increase glucocorticoid levels resulting in increased glucocorticoid receptor (GR) agonism, we tested whether a synthetic GR agonist dexamethasone (Dexa) similarly causes a similar slowdown in whole GI motility. Expectedly, mice dosed with Dexa showed a significant delay in their whole GI motility, when compared to vehicle-treated Control mice (n = 5/cohort; mean ± S.E. of WGTT (in min): Control: 145.0 ± 20.12; Dexa: 214.0 ± 17.49, p = 0.03, Students' t-test; **Fig 2**).

Stress-responsive isoform *VI* is the dominant *Bdnf* isoform expressed in the murine longitudinal muscle - myenteric plexus tissue. We first characterized the expression profile of *Bdnf* in the motility-regulating myenteric plexus tissue of post-natal gut across three ages and in the two sexes. We isolated longitudinal muscle and myenteric plexus (LM-MP) tissue from the ileum of juvenile (1 month), adult (6 month), and aging (17 month) male and female mice (n = 3/sex for 1-month and 6-month-old mice, n = 3 males and 2 females for 17-month-old mice) and performed bulk RNA sequencing. First, we confirmed that *Bdnf* transcripts are detected in the ileal tissues of male and female mice at all ages. We next analyzed whether the stress-responsive *Bdnf IV* (from e4) and *Bdnf VI* (from e6) are expressed in the ileal LM-MP tissue across ages and in the two sexes. We found that at all profiled ages, *Bdnf VI* is the dominant isoform, making up 85.3% (95% CI [81.5%, 89.0%]) of all detected *Bdnf* transcripts (**Fig 3**). Similarly, *Bdnf V* (from e5) expression is detected at all ages and in both male and female tissues (percent representation of *Bdnf V* at 1-month: 9.7%, 6-month: 9.4%, and 17-month: 6.2%). By contrast, the other stress-responsive isoform *Bdnf IV* is detected at 1-month and 6-months of age in both male and female ileal LM-MP (percent representation of *Bdnf IV* at 1-month: 5.3%, and 6-month: 2.3%), but it is not detected in the aging ileal LM-MP – suggesting that the expression of this isoform is reduced or lost with aging. On the other hand, the expression of *Bdnf II* (e2) is not detected at 1-month of

age but is detected at 6-months and 17-months of age (percent representation of *Bdnf II* at 6-month: 3.3%, and 17-month: 5.1%). 6-months age is the only age we queried where we detected the expression of *Bdnf-III* in the murine ileal LM-MP (representing 2.9% of all *Bdnf* transcripts at this age) (**Extended Fig 3-1**). These data show that stress-responsive *Bdnf* isoforms (*IV* and *VI*) represent about or more than 85% of all *Bdnf* transcripts at any age in the murine ileal myenteric plexus.

BDNF and TrkB are expressed by myenteric neurons. Prior data have used immunohistochemical and conditional transgenic mice to establish the expression of BDNF in myenteric ganglia in the post-natal gut (Kovler et al., 2021; Singh et al., 2022). The secreted nature of BDNF and the non-inducible conditional animals used for these experiments have thus left open the question about the exact nature of myenteric cells that express this neurotrophin. By contrast, using a reporter transgenic mouse, have previously shown that TrkB is expressed by myenteric neurons in the adult gut (Nestor-Kalinoski et al., 2022). Here, we use RNAScope to test the expression of transcripts of *Bdnf* and *Ntrk2* (TrkB gene) in the adult murine myenteric plexus. By using RNAScope probes for *Bdnf, Ntrk2*, and the pan-neuronally expressed gene *Tubb3* that were hybridized with fresh-frozen sections of the small intestinal LM-MP tissues, we observed that *Bdnf* and *Ntrk2* transcripts were detected in *Tubb3*$^{+}$ enteric neurons (**Fig 4A**). This data shows that *Bdnf* and *Ntrk2* (TrkB) are neuronally expressed genes in the myenteric plexus. We next performed immunohistochemistry on formalin fixed paraffin embedded (FFPE) tissue sections from the adult small intestine of human patients without any known motility disorder and again found that while BDNF protein was present in the myenteric ganglia, its abundance was significantly higher in neuron-like cells. This again suggests that BDNF is a neuronally expressed protein in the adult myenteric ganglia (**Fig 4B**).

Dexamethasone exposure significantly downregulates myenteric BDNF expression. Since dexamethasone (Dexa), a synthetic glucocorticoid receptor (GR) agonist which mimics the effect of stress-induced increase in cortisol (Dubashynskaya et al., 2021), significantly slows down GI motility (**Fig 2**), we next tested whether exposure to Dexa causes a significant reduction in the expression of stress-responsive *Bdnf IV* and *VI* isoforms. In small intestinal LM-MP of adult male mice treated with Dexa or vehicle, we assessed the abundance of these *Bdnf* at 4 hours post treatment, a timepoint aligning with the duration our WGTT experiments. By performing quantitative real time PCR (qRT-PCR) with isoform-specific TaqMan probes, we found that expression of both *Bdnf IV* and *VI* were significantly reduced in small intestinal LM-MP of mice treated with Dexa when compared to vehicle treated control (n = 3/cohort; mean ± S.E. fold

change of *Bdnf IV*: Control: 1.011 ± 0.104; Dexa: 0.536 ± 0.087, p = 0.025; mean ± S.E. fold change of *Bdnf VI*: Control: 1.012 ± 0.110; Dexa: 0.422 ± 0.042, p = 0.007; Students' t-test; **Fig 5A**).

Bdnf is an immediate early gene whose expression may be triggered by tissue damage (Ballarín et al., 1991; Hughes et al., 1993). To ensure that our results are not affected by the dissection of tissues immediately before RNA isolation, we cultured peeled adult small intestinal LM-MP tissues from male mice in SCM with vehicle (DMSO) or Dex (1 μM) for 4 hours, and again performed qRT-PCR with *Bdnf* isoform-specific probes. Again, we found that exposure to Dex significantly reduced the expression of both stress responsive isoforms *Bdnf IV* and *Bdnf VI* (n = 3/cohort; mean ± S.E. fold change of *Bdnf IV*: Control: 1.002 ± 0.047; Dexa: 0.510 ± 0.099, p = 0.030; mean ± S.E. fold change of *Bdnf VI*: Control: 1.018 ± 0.140; Dexa: 0.520 ± 0.079, p = 0.028; Students' t-test; **Fig 5B**).

Next, we repeated these experiments and used the adult murine small intestinal LM-MP tissues cultured with and without Dex for assessing whether exposure to Dex caused change in BDNF protein levels in tissue. By performing an ELISA, we found that LM-MP cultured with Dex for 4 hours showed significant reduction in the levels of BDNF proteins when compared to LM-MP cultured with vehicle (n = 3/cohort; mean ± S.E. BDNF levels (in pg/g of tissue): Control: 473.0 ± 45.32; Dexa: 85.5 ± 32.63, p = 0.002; Students' t-test; **Fig 5C**).

Targeted activation of TrkB restores motility in Dex-induced delayed transit models. Our observations that reduced *Bdnf* expression is associated with slowed whole gut motility in Dexa-treated mice suggests that the effect of Dexa on whole gut motility may be mediated by a reduced BDNF–TrkB signaling. This would suggest that increasing TrkB signaling would improve gut motility of Dexa-treated mice. To test this hypothesis, we studied whether a synthetic and specific agonist of TrkB can restore whole gut motility of Dexa-treated mice. In rodent models, the serotonin-derived compound HIOC has been demonstrated to be a specific agonist of TrkB (Dhakal et al., 2021). We found that cohorts of mice that were pre-treated with HIOC and then treated with Dexa had significantly lower whole gut transit times on average than Dexa-treated mice that were not treated with HIOC (n = 9/cohort; mean ± S.E. of WGTT (in min): Dexa: 228.3

± 7.12; Dexa + HIOC: 150.0 ± 21.94, p = 0.003, Students' t-test; **Fig 5D**). Of note, we find higher variability in the whole gut transit time in the dual-agonist (Dexa + HIOC) cohort compared to Dexa cohort.

Discussion

Our study establishes that altered BDNF–TrkB signaling in the adult ENS is an important mechanism through which the stress-induced glucocorticoid pathway manifests GI dysmotility. Our study is the first to interrogate the nature of the *Bdnf* isoforms present in the post-natal gut of juvenile, adult, and aging mice, and establishes that at all ages, the stress-responsive (also the glucocorticoid-responsive) isoform *Bdnf VI* is the dominant *Bdnf* isoform expressed in the gut wall. Further, by demonstrating the localization of *Bdnf* and *Ntrk2* transcripts in *Tubb3*-expressing myenteric neurons in the adult murine gut wall, we show that the BDNF–TrkB crosstalk is neuronal in nature. Since stress downregulates the expression of *Bdnf-IV* and *Bdnf-VI* through a glucocorticoid-mediated mechanism, we tested and found that glucocorticoid receptor (GR) agonism (using a synthetic GR agonist dexamethasone) significantly downregulated BDNF expression in the adult LM-MP, and that this was associated with a significant slowdown of intestinal motility. Finally, we established the involvement of the BDNF–TrkB signaling in glucocorticoid-mediated GI dysmotility by showing that TrkB agonism significantly improves GI motility in a mouse model of dexamethasone-induced GI dysmotility. These results together show that GR agonism, an important downstream effect of physiological stress, significantly reduces the expression of *Bdnf-VI* and *IV* isoforms in a subpopulation of myenteric neurons, which results in reduced TrkB signaling in another subpopulation of myenteric neurons to cause GI dysmotility. Promoting TrkB signaling in myenteric neurons thus holds the key to improving GI motility in stress-induced GI dysmotility conditions.

Prior studies have shown that stress and the stress hormone corticotrophin-releasing factor (CRF) in the central nervous system (CNS) induce a slowdown of gastric, small intestinal, and whole gut transit (Zhao et al., 2021; Lobo et al., 2023). Through stimulation of the HPA axis, stress causes increased release of the glucocorticoid cortisol, which has been previously simulated by using the glucocorticoid receptor (GR) agonist dexamethasone. The Thaiss lab demonstrated that GR (*Nr3c1*) is expressed by enteric neurons, and that both stress and dexamethasone similarly slow GI motility (Schneider et al., 2023). Using dexamethasone to simulate the glucocorticoid effect of

404 physiological stress, we identified glucocorticoid-mediated reduction in BDNF–TrkB signaling as
405 a key pathway driving stress-associated GI dysmotility.

406 Alterations and mutations in *Bdnf* and *Ntrk2* have been associated with GI dysmotility (Bonfiglio
407 et al., 2021; Weaver et al., 2022; Linsalata et al., 2023), and exogenous supplementation of BDNF
408 has been observed to have a prokinetic effect in patients (Coulie et al., 2000; Chen et al., 2014).
409 However, the cellular and molecular mechanisms that regulate BDNF levels in these diseases of
410 gut-brain interactions (DGBI) that are often associated with aberrant stress responses were
411 unknown. Our study, which identifies the neuronal nature of BDNF and TrkB and that stress and
412 glucocorticoid-responsive *Bdnf VI* isoform is the most abundant isoform across ages in the post-
413 natal ENS, is the first to establish the mechanism through which this clinically relevant
414 biomolecule is altered in the gut. Previously, the Belgian group (Boesmans et al., 2008) showed
415 that BDNF amplifies neuronal responsiveness of enteric neurons to stimuli, suggesting that this
416 neurotrophin regulates the '*gain*' of TrkB-expressing neurons. These observations, along with our
417 and others' observation of the neuronal nature of TrkB (Boesmans et al., 2008; Nestor-Kalinoski
418 et al., 2022), and our data showing that increasing TrkB signaling in dexamethasone-treated mice
419 improves GI motility suggests that stress-mediated downregulation of BDNF reduces the
420 sensitivity or responsiveness of TrkB-expressing myenteric neurons to cause dysmotility.
421 Together, this identifies that TrkB is an important therapeutic target for the amelioration of GI
422 dysmotility in DGBI patients.

423 It is important to note that while stress-mediated change in glucocorticoid signaling is an important
424 mechanism through which stress manifests dysfunction, stress also drives changes in other
425 hormones in the viscera, which include changes in adrenaline and in the peripheral release of
426 corticotrophin releasing factor (CRF) from mast cells (Kempuraj et al., 2017; Pace and Myers,
427 2023). It is currently unclear how these alternate stress-mediated pathways affect the enteric
428 BDNF–TrkB signaling, and future studies will focus on elucidating this biology further. In addition,
429 our study also identifies important age-associated changes in abundance of *Bdnf* isoforms other
430 than *Bdnf VI*, and future studies will test whether the glucocorticoid-mediated changes in the
431 expression of *Bdnf VI* and other isoforms occurs differentially in an age-associated manner.

432 Thus, by establishing the mechanism through which stress-associated changes in glucocorticoid
433 signaling alters the BDNF–TrkB crosstalk in the adult enteric nervous system, our study provides
434 an important pathway through which stress causes GI dysmotility and provides a putative
435 therapeutic target which can be used for improving GI motility in many DGBI patients.

436 **Transcriptomic Data and Code availability**: Transcriptomic Data and Code availability: All the
437 transcriptomic data has been deposited in GEO GSE284108 and the code for analysis is
438 deposited in Github at https://github.com/jaredslosberg/timecourse_lmmp_bulkrnaseq/

439 **Acknowledgements**

440 We acknowledge Dr. Xia Qian (Dept of Pathology, BIDMC) and Mrs. Vilmonse (Eva) Csizmadia
441 (Dept of Anesthesia, BIDMC) for their help. The authors would like to thank the Neurobiology
442 Imaging Facility (NIF) at Harvard Medical School, Boston, MA for performing the RNAscope
443 assay. This work was supported by funding from NIA R01AG66768, R21AG072107, Diacomp
444 Foundation (Pilot award Augusta University) and Pilot grant from the Harvard Digestive Disease
445 Core (SK). This work was also supported by funding from the Maryland Genetics, Epidemiology,
446 and Medicine training program sponsored by the Burroughs Welcome Fund (JS) and from Walter
447 Benjamin Fellowship (528835020) from Deutsche Forschungsgemeinschaft (PS).

448

Figures:

Figure 1. Restraint stress significantly increases whole gut transit time in adult male mice. Graphical representation of the mean ± standard error of the whole gut transit times (assayed using the carmine-red dye method) of two cohorts of mice, where the mice in the 'Stress' cohort were restrained for an hour every day for 5 days, and the 'Control' cohort mice were handled similarly but not restrained. Mice in the Stress cohort showed significantly longer whole gut transit times on average than mice in the control cohort. *$p < 0.05$. Student's t-test.

Figure 2. Dexamethasone treatment significantly increases whole gut transit time in adult male mice. Graphical representation of the mean ± standard error of the whole gut transit times (assayed using the carmine-red dye method) of two cohorts of mice, where the mice in the 'Dexa' cohort were dosed once with dexamethasone (5mg/Kg body weight), and the 'Control' cohort mice were dosed with Vehicle (10% DMSO in Saline). Mice in the Dexa cohort showed significantly longer whole gut transit times on average than mice in the control cohort. *$p < 0.05$. Student's t-test.

Figure 3. *Bdnf VI* is the dominant *Bdnf* isoform in the ileal LM-MP at all post-natal ages. Graphical representation of the proportions of various *Bdnf* isoforms whose transcripts were detected in the murine ileal LM-MP layer in two different sexes across three different ages of 1-month (juvenile), 6-month (mature adult), and 17-month (aging). This representation shows that stress-responsive *Bdnf VI* is the dominant isoform found in the murine ileal LM-MP at all ages, with its proportions accounting for >80% of all isoforms. The isoform *Bdnf V* is the second most represented isoform at all ages in the murine LM-MP layer but little is known about the mechanisms that regulate its expression. In addition to *Bdnf VI, Bdnf IV* is another stress-responsive isoform detected in the juvenile and adult mice but is not detected in aging murine ileal LM-MP. In contrast to *Bdnf IV, Bdnf II* isoform is detected in the adult and aging ileal tissues, but not in the juvenile tissues. Finally, *Bdnf III* isoform is detected only in the adult ileal LM-MP and not at the other ages.

Extended Figure 3 – 1: **Gene and isoform expression of *Bdnf* by age**. (A) *Bdnf* expression is detected in 1-month, 6-month, and 17-month-old mice. Isoform-level abundance estimates were collapsed to gene-level after inter-library normalization with edgeR (TMM method). Across all ages, average expression of *Bdnf* is 0.38 ± 0.02 TPM. Independently, gene-level differential expression across age was conducted with DESeq2 (counts ~ age + RIN + batch, Wald test) and *Bdnf* was not identified as differential by age across any comparison. (B) Abundance estimates of individual *Bdnf* isoforms identify the e6 isoform (ENSMUST00000111045) as the majority

isoform in each condition. The average expression of this isoform is 0.32 ± 0.08 TPM. Other lowly detected isoforms include e5 (ENSMUST00000176893), e4 (ENSMUST00000111050), e3 (ENSMUST00000111046), and e2 (ENSMUST00000111047), while remaining isoforms were not detected. Differential isoform usage by age was tested via the DEXSeq wrapper within IsoformSwitchAnalyzeR (Likelihood ratio test, full model: ~ sample + exon + age:exon, reduced model: ~ sample + exon). No *Bdnf* isoforms were identified as having significant differential usage by age. (C) Isoform level expression was transformed to isoform fraction (IF) measures by age (for each age, sum of IF's is 1).

Figure 4. *Bdnf* is a neuronally expressed gene in the adult murine small intestinal ENS. Transcriptomic and proteomic evidence of neuronal expression of BDNF. (A) Confocal microscopy image of a 14 µm thick section of adult murine ileal LM-MP tissue which was probed with RNAScope-probes against all *Bdnf* (green)*, Ntrk2* (red) transcripts and against the pan-neuronal *Tubb3* (grey) transcript show that off (i, ii) all the *Tubb3*-expressing myenteric neurons, distinct neurons express *Bdnf* (yellow arrow, (i, iii)) and *Ntrk2* (TrkB, red arrow, (i, iv)). That *Bdnf* and *Ntrk2* expressing neurons are distinct neurons can also be observed in (v) an image representation where the dominant *Tubb3* transcripts are not visualized. No other cellular subset inside or outside the ganglia shows expression of *Bdnf* or *Ntrk2* transcripts providing evidence that BDNF and TrkB in the adult small intestine are neuronally restricted. Nuclei are labeled with DAPI (blue). Scale bar represents 10 µm. (B) Immunostaining a human small intestinal tissue section with antibodies against BDNF also shows that while the secreted form of BDNF is present inside and outside of the myenteric ganglia, the highly enriched presence of BDNF in the cytoplasm of a myenteric neuron (black arrow) suggests its likely source of expression. Scale bar represents 100 µm.

Figure 5. Dexamethasone causes a significant reduction in the abundance of enteric BDNF to drive GI dysmotility. (A) Adult male mice dosed with dexamethasone (Dexa) and sacrificed 4 hours later showed a significant down regulation in the expression of stress and glucocorticoid-responsive *Bdnf IV* and *Bdnf VI* transcripts in their small intestinal LM-MP tissues, when compared to age- and sex-matched mice that were dosed with vehicle. *p < 0.05, **p < 0.01, Students' t-test. (B) Small intestinal LM-MP tissues from adult male mice that were cultured with Dexa for 4 hours showed a significant down regulation in the expression of stress and glucocorticoid-responsive *Bdnf IV* and *Bdnf VI* transcripts in their small intestinal LM-MP tissues, when compared to tissues from age- and sex-matched mice that were cultured with vehicle. *p < 0.05, Students' t-test. (C) Small intestinal LM-MP tissues from adult male mice that were cultured with Dexa for 4

514 hours showed a significant reduction in the abundance of BDNF protein as assessed by ELISA,
515 when compared to tissues from age- and sex-matched mice that were cultured with vehicle. **p
516 < 0.01, Students' t-test. (D) Dexa-treated adult male mice that were also dosed with the synthetic
517 and specific agonist of TrkB HIOS showed significant reduction in their whole gut transit time of
518 orally gavaged carmine-red dye, and hence improved gut motility, when compared to age- and
519 sex-matched mice that were dosed only with Dexa.

520

521 **Table 1**

Resource	**Vendor**	**Cat. No.**
BDNF antibody	Abcam	Ab108319
Bdnf RNAScope assay	RNAScope, ACD-Bio	457761
Ntrk2 RNAScope assay	RNAScope, ACD-Bio	423611-C2
Tubb3 RNAScope assay	RNAScope, ACD-Bio	423391-C3
TaqMan Primers & Probes		
Target	**Sequence/Cat. No.**	**Company**
Bdnf IV Fwd	CGTTTACTTCTTTCATGGGCG	IDT
Bdnf IV Rev	AGCTGCCTTGATGTTTACTTTG	IDT
Bdnf IV probe	56-FAM/AGGATGGTC/ZEN/ATCACTCTTCTCACCTGG/3IABkFQ	IDT
Bdnf VI Fwd	ATGCAACCGAAGTATGAAATAACC	IDT
Bdnf VI Rev	GGACCAGAAGCGTGACAAC	IDT
Bdnf VI probe	56-FAM/ACCAGGTGA/ZEN/GAAGAGTGATGACCATCC/3IBkFQ	IDT
Hprt TaqMan assay	Mm00446966_m1	Invitrogen

522

523

524

525

526

References:

Aid T, Kazantseva A, Piirsoo M, Palm K, Timmusk T (2007) Mouse and rat BDNF gene structure and expression revisited. J Neurosci Res 85:525-535.

Ballarín M, Ernfors P, Lindefors N, Persson H (1991) Hippocampal damage and kainic acid injection induce a rapid increase in mRNA for BDNF and NGF in the rat brain. Experimental Neurology 114:35-43.

Begni V, Riva Marco A, Cattaneo A (2016) Cellular and molecular mechanisms of the brain-derived neurotrophic factor in physiological and pathological conditions. Clinical Science 131:123-138.

Boesmans W, Gomes P, Janssens J, Tack J, Vanden Berghe P (2008) Brain-derived neurotrophic factor amplifies neurotransmitter responses and promotes synaptic communication in the enteric nervous system. Gut 57:314-322.

Bonfiglio F et al. (2021) GWAS of stool frequency provides insights into gastrointestinal motility and irritable bowel syndrome. Cell Genom 1:None.

Chalazonitis A, Li Z, Pham TD, Chen J, Rao M, Lindholm P, Saarma M, Lindahl M, Gershon MD (2020) Cerebral dopamine neurotrophic factor is essential for enteric neuronal development, maintenance, and regulation of gastrointestinal transit. J Comp Neurol 528:2420-2444.

Chen F, Yu Y, Wang P, Dong Y, Wang T, Zuo X, Li Y (2014) Brain-derived neurotrophic factor accelerates gut motility in slow-transit constipation. Acta Physiol (Oxf) 212:226-238.

Chen FX, Yu YB, Yuan XM, Zuo XL, Li YQ (2012) Brain-derived neurotrophic factor enhances the contraction of intestinal muscle strips induced by SP and CGRP in mice. Regul Pept 178:86-94.

Chen H, Lombes M, Le Menuet D (2017) Glucocorticoid receptor represses brain-derived neurotrophic factor expression in neuron-like cells. Mol Brain 10:12.

Coulie B, Szarka LA, Camilleri M, Burton DD, McKinzie S, Stambler N, Cedarbaum JM (2000) Recombinant human neurotrophic factors accelerate colonic transit and relieve constipation in humans. Gastroenterology 119:41-50.

Dhakal S, He L, Lyuboslavsky P, Sidhu C, Chrenek MA, Sellers JT, Boatright JH, Geisert EE, Setterholm NA, McDonald FE, Iuvone PM (2021) A Tropomycin-Related Kinase B Receptor Activator for the Management of Ocular Blast-Induced Vision Loss. J Neurotrauma 38:2896-2906.

Dubashynskaya NV, Bokatyi AN, Skorik YA (2021) Dexamethasone Conjugates: Synthetic Approaches and Medical Prospects. Biomedicines 9.

Hill JL, Martinowich K (2016) Activity-dependent signaling: influence on plasticity in circuits controlling fear-related behavior. Curr Opin Neurobiol 36:59-65.

Hong EJ, McCord AE, Greenberg ME (2008) A biological function for the neuronal activity-dependent component of Bdnf transcription in the development of cortical inhibition. Neuron 60:610-624.

Hughes P, Beilharz E, Gluckman P, Dragunow M (1993) Brain-derived neurotrophic factor is induced as an immediate early gene following N-methyl-d-aspartate receptor activation. Neuroscience 57:319-328.

569 Kempuraj D, Selvakumar GP, Thangavel R, Ahmed ME, Zaheer S, Raikwar SP, Iyer SS, Bhagavan
570 SM, Beladakere-Ramaswamy S, Zaheer A (2017) Mast Cell Activation in Brain Injury,
571 Stress, and Post-traumatic Stress Disorder and Alzheimer's Disease Pathogenesis. Front
572 Neurosci 11:703.
573 Konturek TJ, Martinez C, Niesler B, van der Voort I, Mönnikes H, Stengel A, Goebel-Stengel M
574 (2020) The Role of Brain-Derived Neurotrophic Factor in Irritable Bowel Syndrome. Front
575 Psychiatry 11:531385.
576 Kovler ML, Gonzalez Salazar AJ, Fulton WB, Lu P, Yamaguchi Y, Zhou Q, Sampah M, Ishiyama A,
577 Prindle T, Jr., Wang S, Jia H, Wipf P, Sodhi CP, Hackam DJ (2021) Toll-like receptor 4-
578 mediated enteric glia loss is critical for the development of necrotizing enterocolitis. Sci
579 Transl Med 13:eabg3459.
580 Kulkarni S et al. (2017) Adult enteric nervous system in health is maintained by a dynamic
581 balance between neuronal apoptosis and neurogenesis. Proc Natl Acad Sci U S A
582 114:E3709-e3718.
583 Leigh S-J, Uhlig F, Wilmes L, Sanchez-Diaz P, Gheorghe CE, Goodson MS, Kelley-Loughnane N,
584 Hyland NP, Cryan JF, Clarke G (2023) The impact of acute and chronic stress on
585 gastrointestinal physiology and function: a microbiota–gut–brain axis perspective. The
586 Journal of Physiology 601:4491-4538.
587 Linsalata M, Prospero L, Riezzo G, Orlando A, D'Attoma B, Ignazzi A, Russo F (2023) Somatization
588 is associated with altered serum levels of vitamin D, serotonin, and brain-derived
589 neurotrophic factor in patients with predominant diarrhea irritable bowel syndrome.
590 Neurogastroenterol Motil 35:e14512.
591 Linz R, Puhlmann LMC, Apostolakou F, Mantzou E, Papassotiriou I, Chrousos GP, Engert V, Singer
592 T (2019) Acute psychosocial stress increases serum BDNF levels: an antagonistic relation
593 to cortisol but no group differences after mental training. Neuropsychopharmacology
594 44:1797-1804.
595 Liu S (2018) Neurotrophic factors in enteric physiology and pathophysiology. Neurogastroenterol
596 Motil 30:e13446.
597 Lobo B, Tramullas M, Finger BC, Lomasney KW, Beltran C, Clarke G, Santos J, Hyland NP, Dinan
598 TG, Cryan JF (2023) The Stressed Gut: Region-specific Immune and Neuroplasticity
599 Changes in Response to Chronic Psychosocial Stress. J Neurogastroenterol Motil 29:72-
600 84.
601 Martinowich K, Manji H, Lu B (2007) New insights into BDNF function in depression and anxiety.
602 Nat Neurosci 10:1089-1093.
603 Murakami S, Imbe H, Morikawa Y, Kubo C, Senba E (2005) Chronic stress, as well as acute stress,
604 reduces BDNF mRNA expression in the rat hippocampus but less robustly. Neurosci Res
605 53:129-139.
606 Nestor-Kalinoski A, Smith-Edwards KM, Meerschaert K, Margiotta JF, Rajwa B, Davis BM, Howard
607 MJ (2022) Unique Neural Circuit Connectivity of Mouse Proximal, Middle, and Distal
608 Colon Defines Regional Colonic Motor Patterns. Cell Mol Gastroenterol Hepatol 13:309-
609 337.e303.
610 Pace SA, Myers B (2023) Hindbrain Adrenergic/Noradrenergic Control of Integrated Endocrine
611 and Autonomic Stress Responses. Endocrinology 165.

Pruunsild P, Sepp M, Orav E, Koppel I, Timmusk T (2011) Identification of cis-elements and transcription factors regulating neuronal activity-dependent transcription of human BDNF gene. J Neurosci 31:3295-3308.

Qin HY, Cheng CW, Tang XD, Bian ZX (2014) Impact of psychological stress on irritable bowel syndrome. World J Gastroenterol 20:14126-14131.

Russell G, Lightman S (2019) The human stress response. Nature Reviews Endocrinology 15:525-534.

Schneider KM et al. (2023) The enteric nervous system relays psychological stress to intestinal inflammation. Cell 186:2823-2838.e2820.

Sharkey KA, Mawe GM (2023) The enteric nervous system. Physiol Rev 103:1487-1564.

Singh A, Singh J, Rattan S (2022) Evidence for the presence and release of BDNF in the neuronal and non-neuronal structures of the internal anal sphincter. Neurogastroenterology & Motility 34:e14099.

Singh A, Mohanty I, Singh J, Rattan S (2020) BDNF augments rat internal anal sphincter smooth muscle tone via RhoA/ROCK signaling and nonadrenergic noncholinergic relaxation via increased NO release. Am J Physiol Gastrointest Liver Physiol 318:G23-g33.

Sperber AD et al. (2021) Worldwide Prevalence and Burden of Functional Gastrointestinal Disorders, Results of Rome Foundation Global Study. Gastroenterology 160:99-114.e113.

Tsankova NM, Berton O, Renthal W, Kumar A, Neve RL, Nestler EJ (2006) Sustained hippocampal chromatin regulation in a mouse model of depression and antidepressant action. Nat Neurosci 9:519-525.

Wang F, Flanagan J, Su N, Wang LC, Bui S, Nielson A, Wu X, Vo HT, Ma XJ, Luo Y (2012) RNAscope: a novel in situ RNA analysis platform for formalin-fixed, paraffin-embedded tissues. J Mol Diagn 14:22-29.

Weaver KR, Mustapic M, Kapogiannis D, Henderson WA (2022) Neuronal-enriched extracellular vesicles in individuals with IBS: A pilot study of COMT and BDNF. Neurogastroenterol Motil 34:e14257.

Wood JD (2016) Enteric Nervous System: Neuropathic Gastrointestinal Motility. Digestive Diseases and Sciences 61:1803-1816.

Zhang Y, Bi YX, Chen J, Li S, Wu XX, Zhang L, Lin ZJ, Han S, Ding SZ (2021) Association of Peroxiredoxin 1 and brain-derived neurotrophic factor serum levels with depression and anxiety symptoms in patients with irritable bowel syndrome. Gen Hosp Psychiatry 68:59-64.

Zhao Y-X, Cui C-X, Gao J-H, Liu J, Liu Q, Lu F-Y, Xin J-J, Yu X-C, Zhu B (2021) Electroacupuncture ameliorates corticotrophin-releasing factor-induced jejunal dysmotility in a rat model of stress. Acupuncture in Medicine 39:135-145.

Zheng Z, Liu Y, Mu R, Guo X, Feng Y, Guo C, Yang L, Qiu W, Zhang Q, Yang W, Dong Z, Qiu S, Dong Y, Cui Y (2024) A small population of stress-responsive neurons in the hypothalamus-habenula circuit mediates development of depression-like behavior in mice. Neuron.

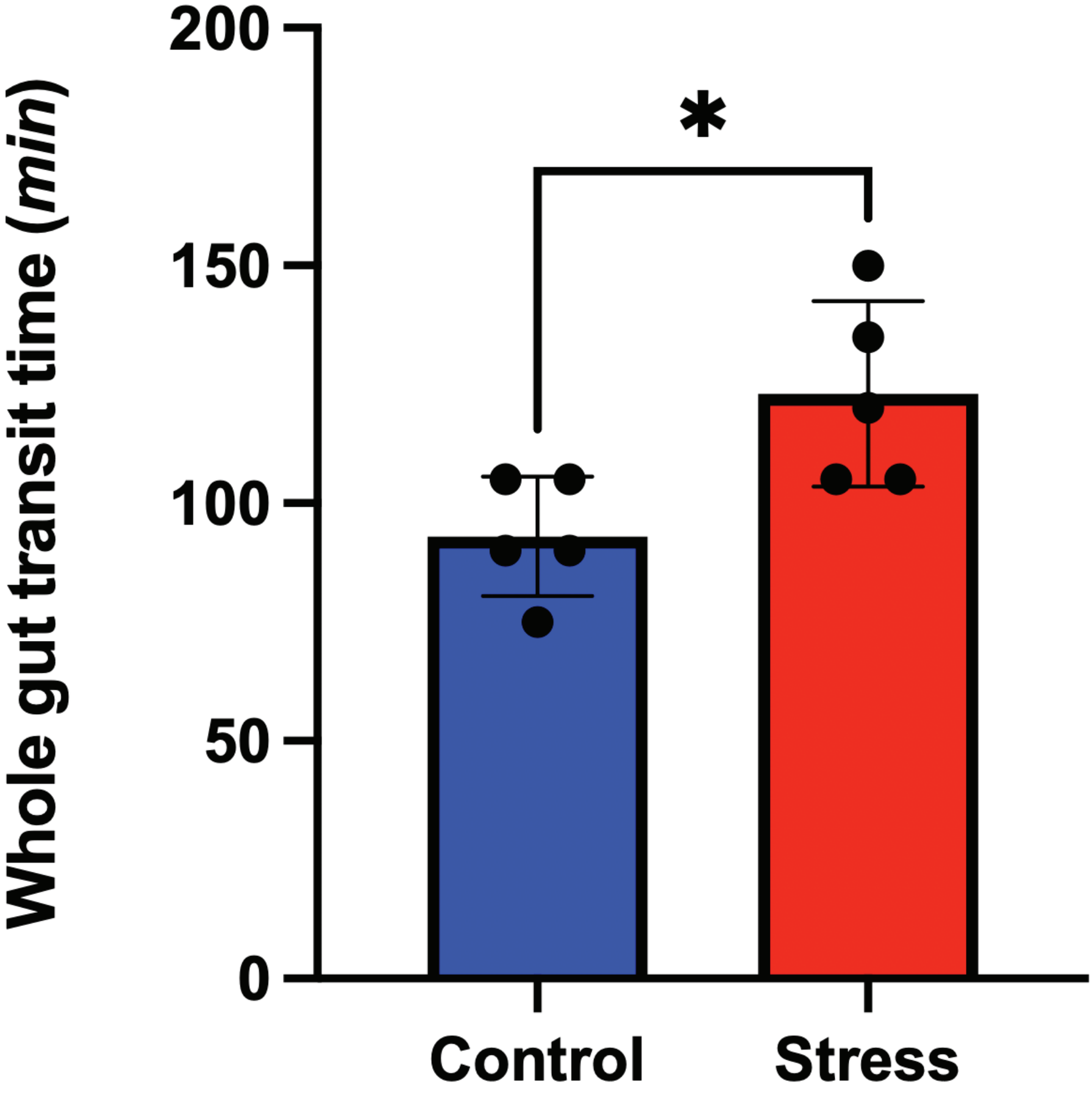
Whole gut transit time (min)
200
150
100
50
0
*
Control
Stress

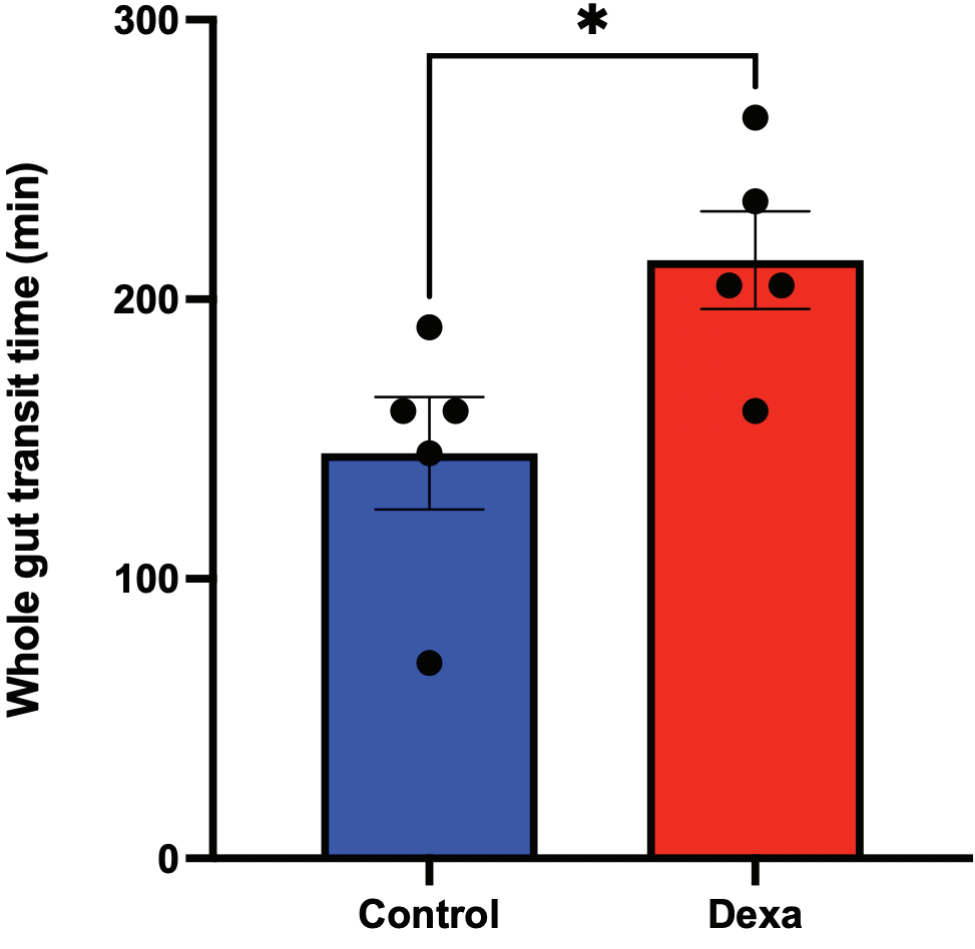
300
200
100
0
Whole gut transit time (min)
*
Control
Dexa

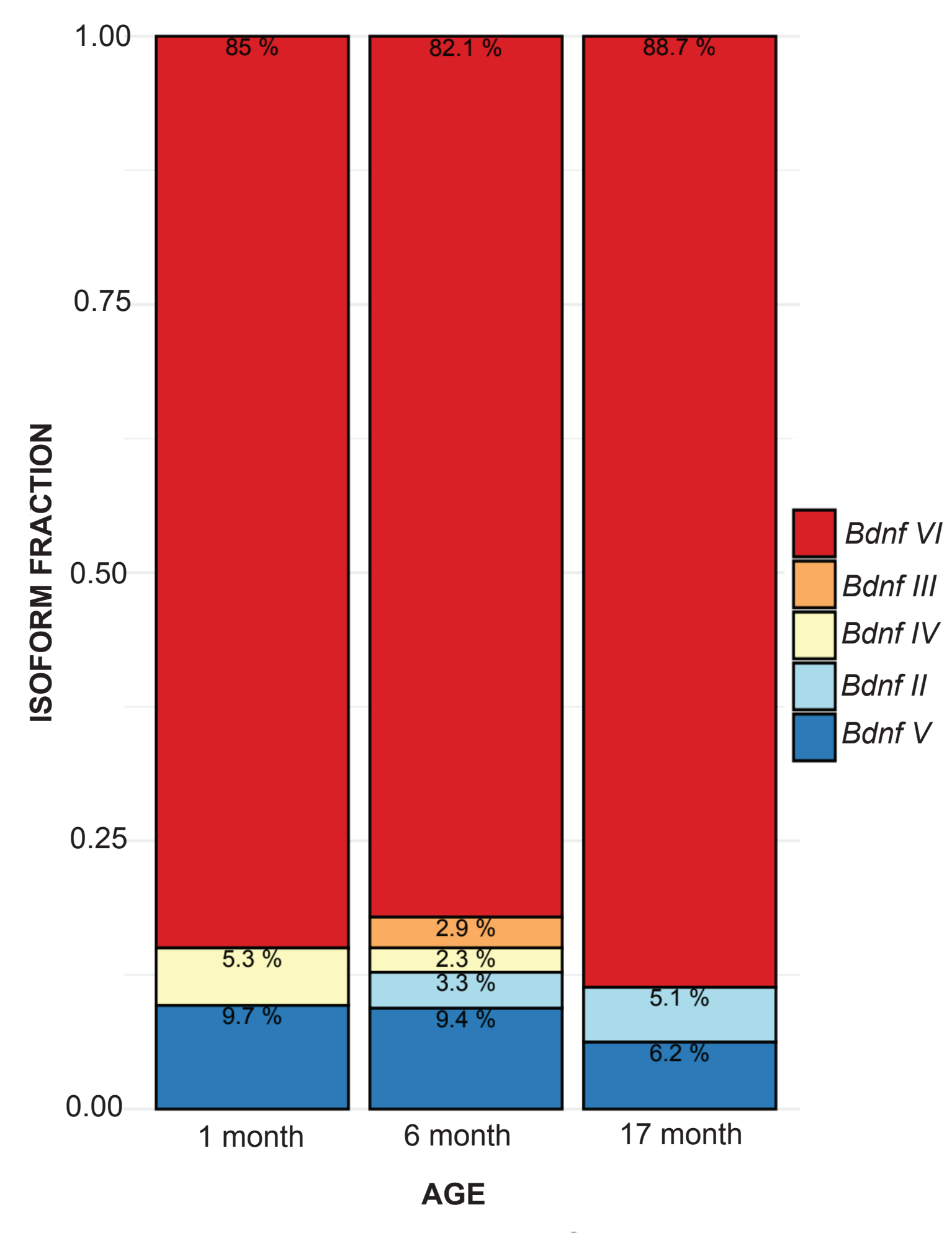
1.00
0.75
0.50
0.25
0.00
ISOFORM FRACTION
85 %
82.1 %
88.7 %
5.3 %
2.9 %
2.3 %
3.3 %
9.7 %
9.4 %
5.1 %
6.2 %
1 month
6 month
17 month
AGE
Bdnf VI
Bdnf III
Bdnf IV
Bdnf II
Bdnf V

1 month 6 month 17 month

AGE

A

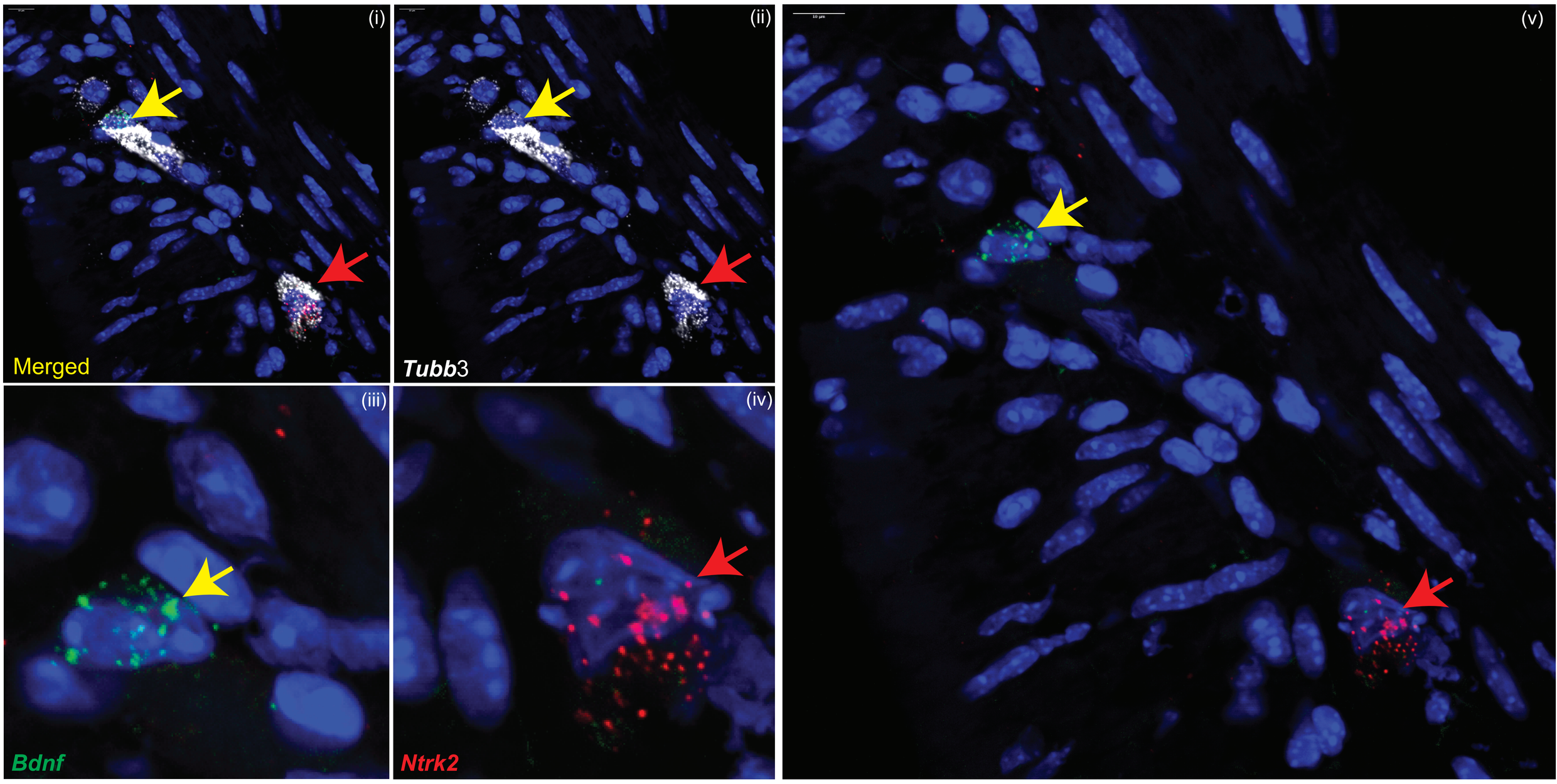

B

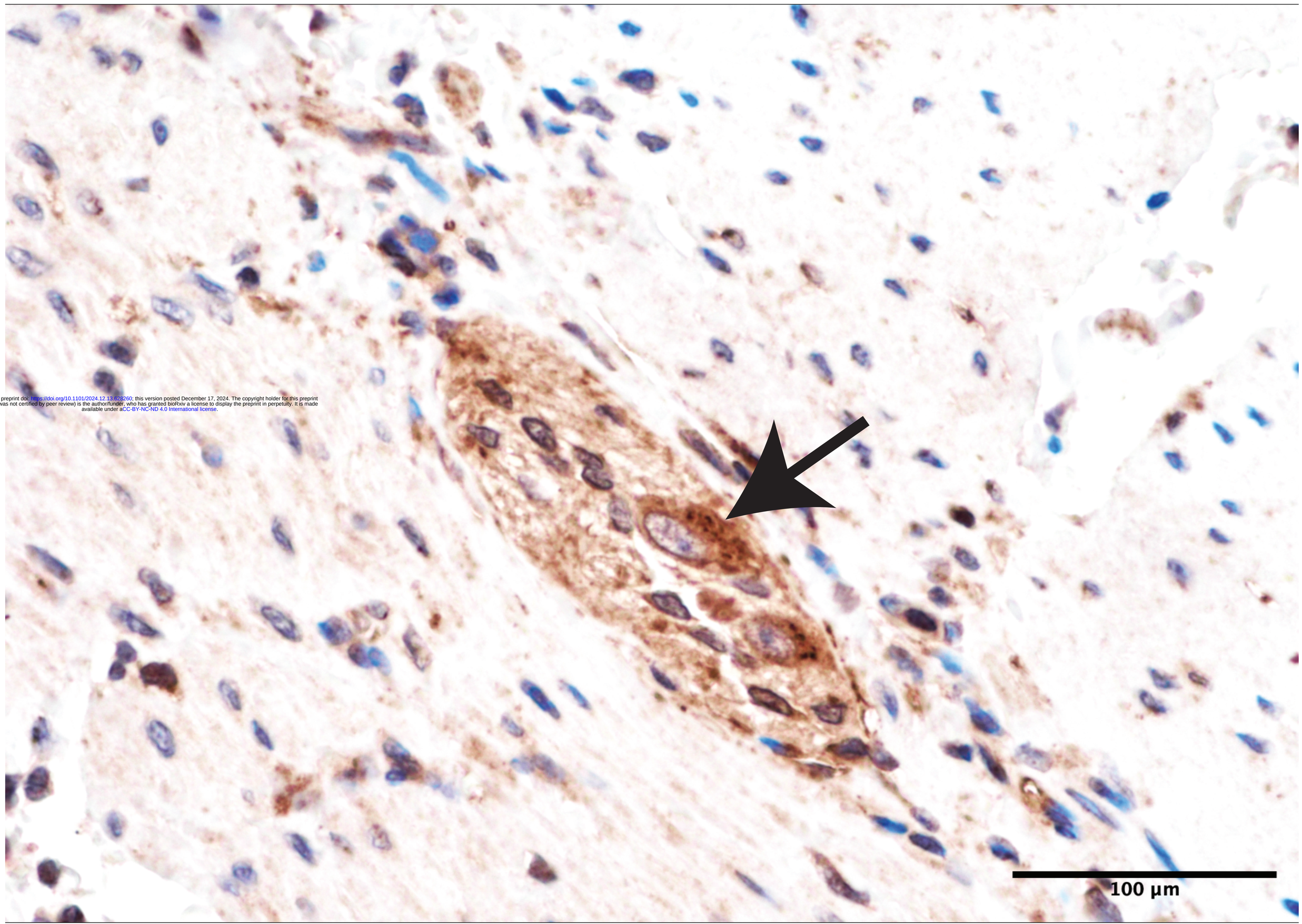

A

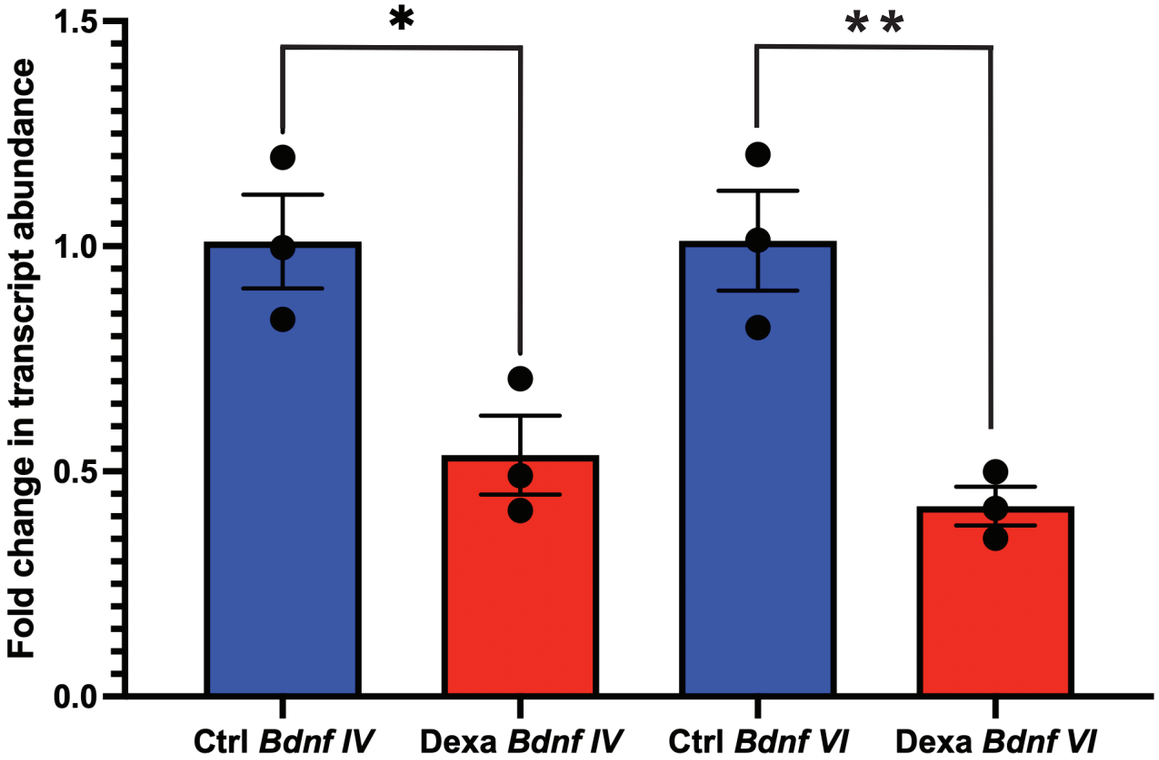
Fold change in transcript abundance
1.5
1.0
0.5
0.0
*
**
Ctrl Bdnf IV
Dexa Bdnf IV
Ctrl Bdnf VI
Dexa Bdnf VI

B

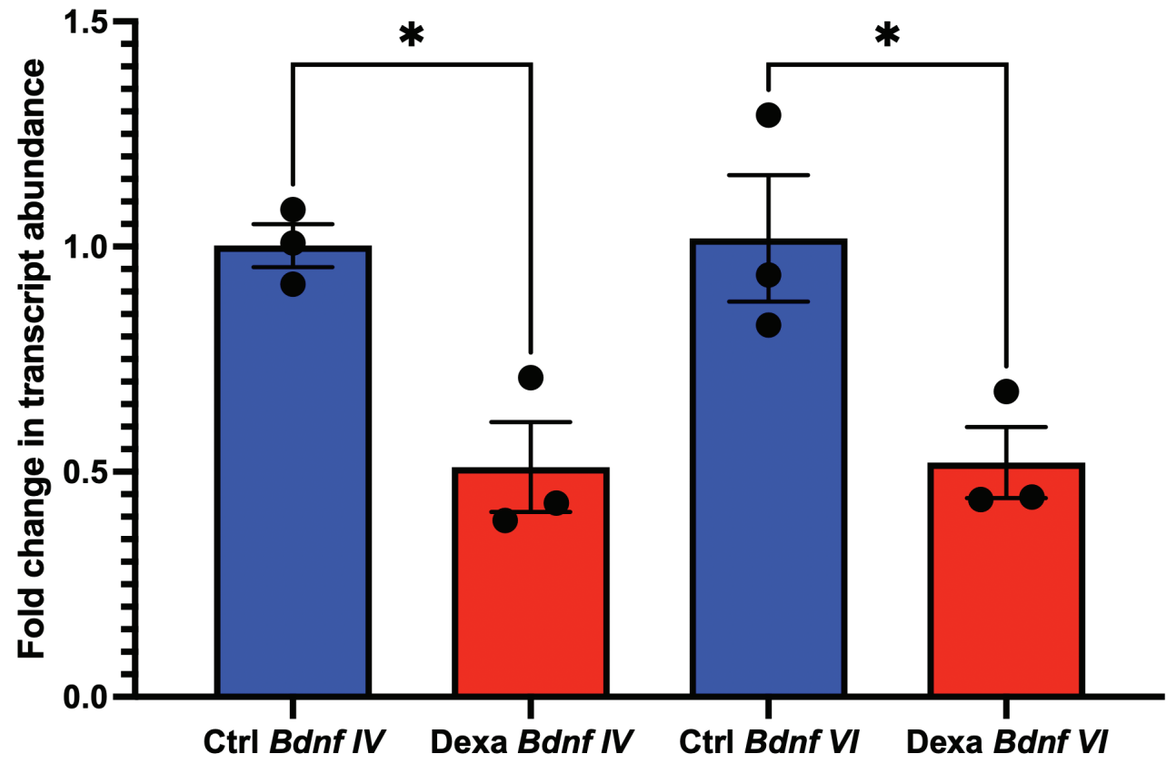
Fold change in transcript abundance
1.5
1.0
0.5
0.0
*
*
Ctrl Bdnf IV
Dexa Bdnf IV
Ctrl Bdnf VI
Dexa Bdnf VI

C

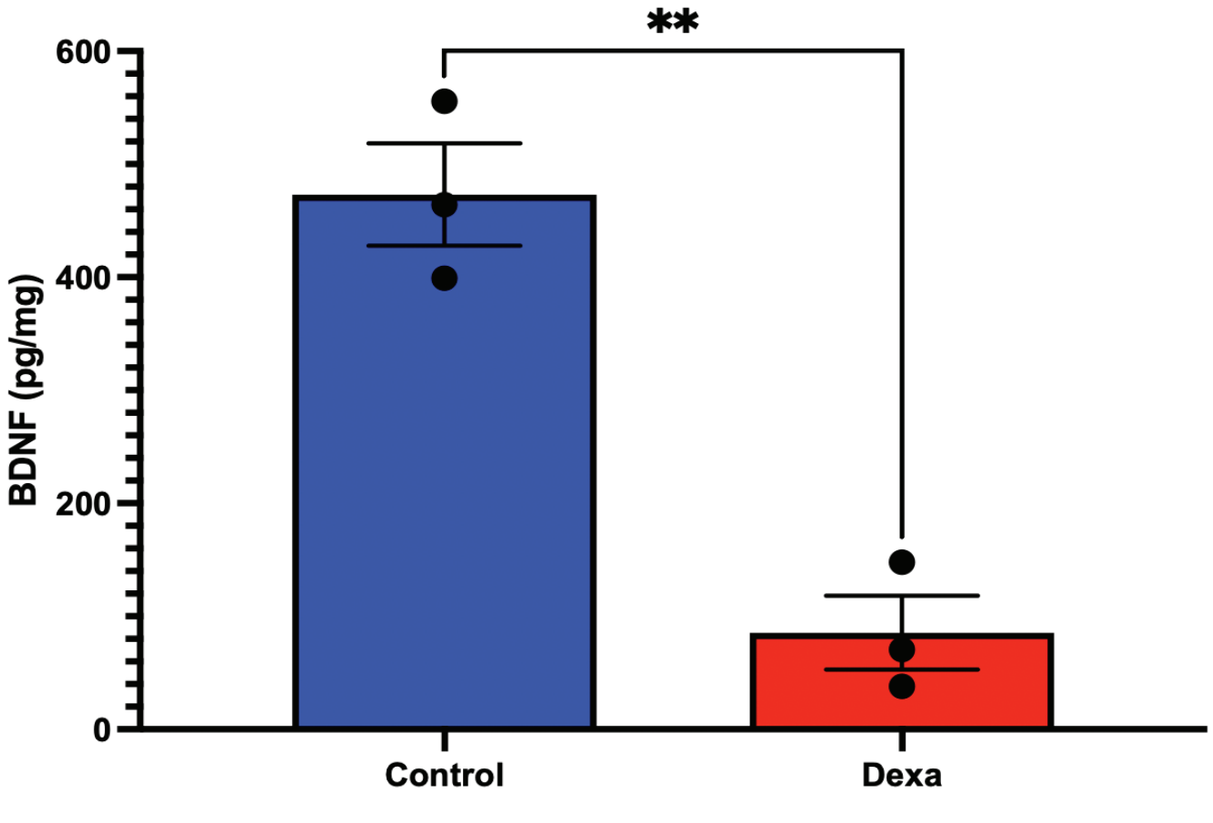
BDNF (pg/mg)
600
400
200
0
**
Control
Dexa

D

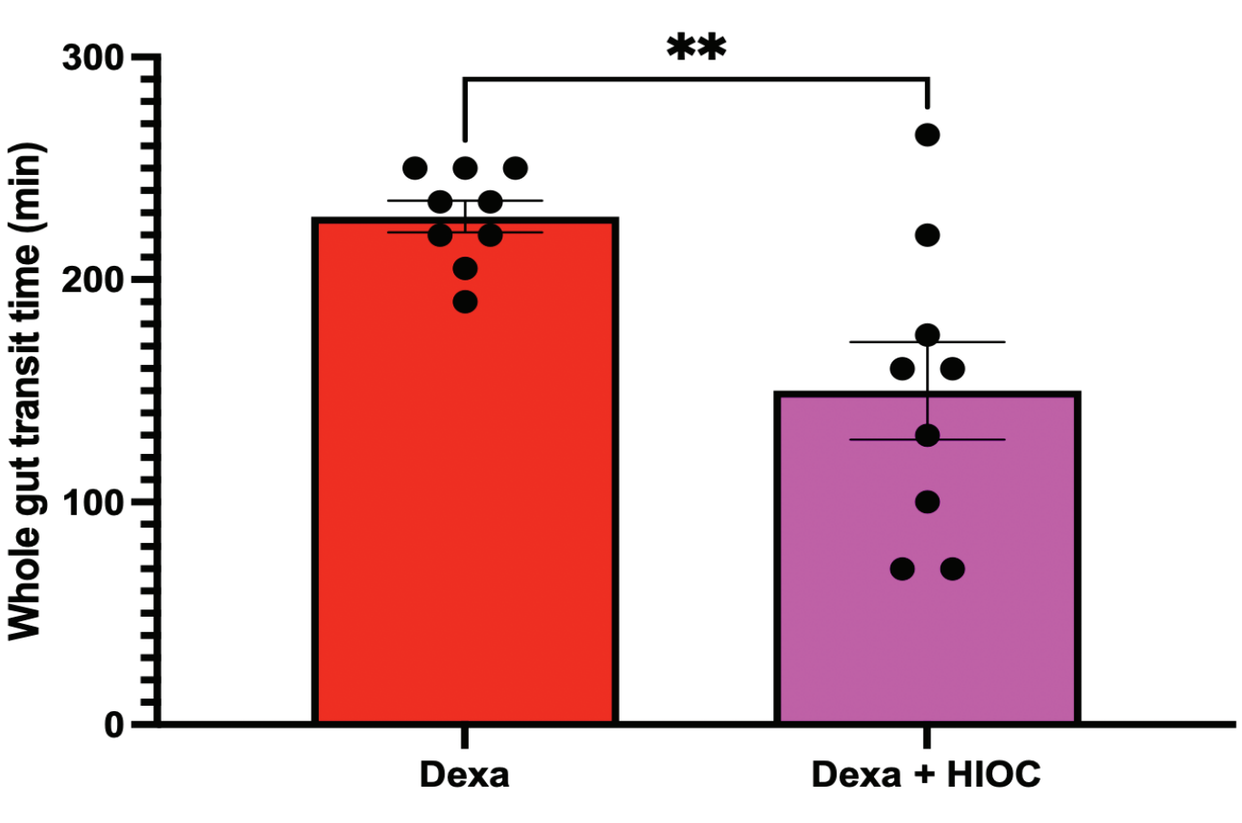
Whole gut transit time (min)
300
200
100
0
**
Dexa
Dexa + HIOC